npj regenerative medicine

www.nature.com/npjregenmed

ARTICLE OPEN

Check for updates

Endogenous tenocyte activation underlies the regenerative capacity of the adult zebrafish tendon

Stephanie L. Tsai[1], Steffany Villaseñor[1], Rishita R. Shah[2] and Jenna L. Galloway[1,3]✉

Tendons are essential, frequently injured connective tissues that transmit forces from muscle to bone. Their unique highly ordered, matrix-rich structure is critical for proper function. While adult mammalian tendons heal after acute injuries, endogenous tendon cells, or tenocytes, fail to respond appropriately, resulting in the formation of disorganized fibrovascular scar tissue with impaired function and increased propensity for re-injury. Here, we show that, unlike mammals, adult zebrafish tenocytes activate upon injury and fully regenerate the tendon. Using a full tear injury model in the adult zebrafish craniofacial tendon, we defined the hallmark stages and cellular basis of tendon regeneration through multiphoton imaging, lineage tracing, and transmission electron microscopy approaches. Remarkably, we observe that zebrafish tendons regenerate and restore normal collagen matrix ultrastructure by 6 months post-injury (mpi). Tendon regeneration progresses in three main phases: inflammation within 24 h post-injury (hpi), cellular proliferation and formation of a cellular bridge between the severed tendon ends at 3–5 days post-injury (dpi), and re-differentiation and matrix remodeling beginning from 5 dpi to 6 mpi. Importantly, we demonstrate that pre-existing tenocytes are the main cellular source of regeneration, proliferating and migrating upon injury to ultimately bridge the tendon ends. Finally, we show that TGF-β signaling is required for tenocyte recruitment and bridge formation. Collectively, our work debuts and aptly positions the adult zebrafish tendon as an invaluable comparative system to elucidate regenerative mechanisms that may inspire new therapeutic strategies.

npj Regenerative Medicine (2023)8:52 ; https://doi.org/10.1038/s41536-023-00328-w

INTRODUCTION

Tendons are highly specialized structures that connect and transmit forces from muscle to bone, enabling movement. Compared to other tissues, tendons are relatively hypocellular. The mass of the tendon is predominantly comprised of a dense extracellular matrix composed of highly aligned type I collagen fibers running uniaxially from the myotendinous junction (MTJ) through the midbody to the tendon-bone attachment, or enthesis. Deeply embedded within the matrix are organized arrays of tendon cells, or tenocytes, which are elongated, stellate-shaped cells with long processes that form an intricate network with neighboring cells via gap junctions[1–3]. While tendons can vary in size and morphology, the highly aligned matrix and tenocyte network are stable features universally required for efficient force transmission and mechanotransduction along the length of the tendon[4–6].

As tendons play a pivotal role in everyday movement, they are frequently injured. Unfortunately, the unique, highly ordered tissue architecture cannot be restored in mammals post-injury. Severe tendon injuries including full tears result in the formation of disorganized fibrovascular scar tissue with impaired function and a higher likelihood of both re-injury as well as developing joint degenerative conditions[7]. Although injuries to tendons and other joint connective tissues are estimated to account for 45% of all musculoskeletal injuries, effective treatments are limited and often result in surgical intervention, which is costly and variable in success[8–10]. Better therapeutic strategies to treat tendon injuries are needed in the clinic to improve patient quality of life as well as ameliorate a mounting healthcare burden.

To this end, most research efforts have been largely focused on understanding the mechanisms underlying adult mammalian fibrotic tendon healing to identify new therapeutic strategies to augment existing clinical treatments. Yet, important lessons on how to achieve tendon regeneration rather than scarring can be learned from natural examples that have been recently reported including in neonatal mice[11–13] and larval zebrafish[14]. These tendon regenerative models can serve as powerful systems to identify mechanisms required for tendon regeneration which may ultimately accelerate the advancement of clinical strategies. However, the previous studies in zebrafish and mice are examples of regeneration set during developmental stages in which the tendon is still actively growing and maturing[15,16]. As cellular plasticity is higher during tissue formation, the mechanisms directing neonatal or larval regeneration may differ between development and adulthood. An adult tendon regenerative model would therefore be invaluable to the field as a comparative paradigm to understand mechanisms driving proper regeneration.

While mammalian regenerative capacity declines from embryonic and postnatal stages to adulthood, zebrafish retain the remarkable ability to regenerate various tissues and organs as adults including their heart and spinal cord[17]; however, tendon regeneration has yet to be examined. Here, we demonstrate that adult zebrafish regenerate their tendon following full transection. We delineate hallmark processes of tendon regeneration, reveal that pre-existing tenocytes are the main cellular source of regenerated tendon tissue, and show that TGF-β signaling is required for regeneration.

RESULTS

The adult zebrafish tendon can regenerate after acute injury

To determine if adult zebrafish tendons regenerate, we performed full transection injuries on the craniofacial maxillary superficial

[1]Center for Regenerative Medicine, Department of Orthopaedic Surgery, Massachusetts General Hospital, Harvard Medical School, Boston, MA, USA. [2]Department of Biology, Barnard College, New York, NY, USA. [3]Harvard Stem Cell Institute, Cambridge, MA, USA. ✉email: jgalloway@mgh.harvard.edu

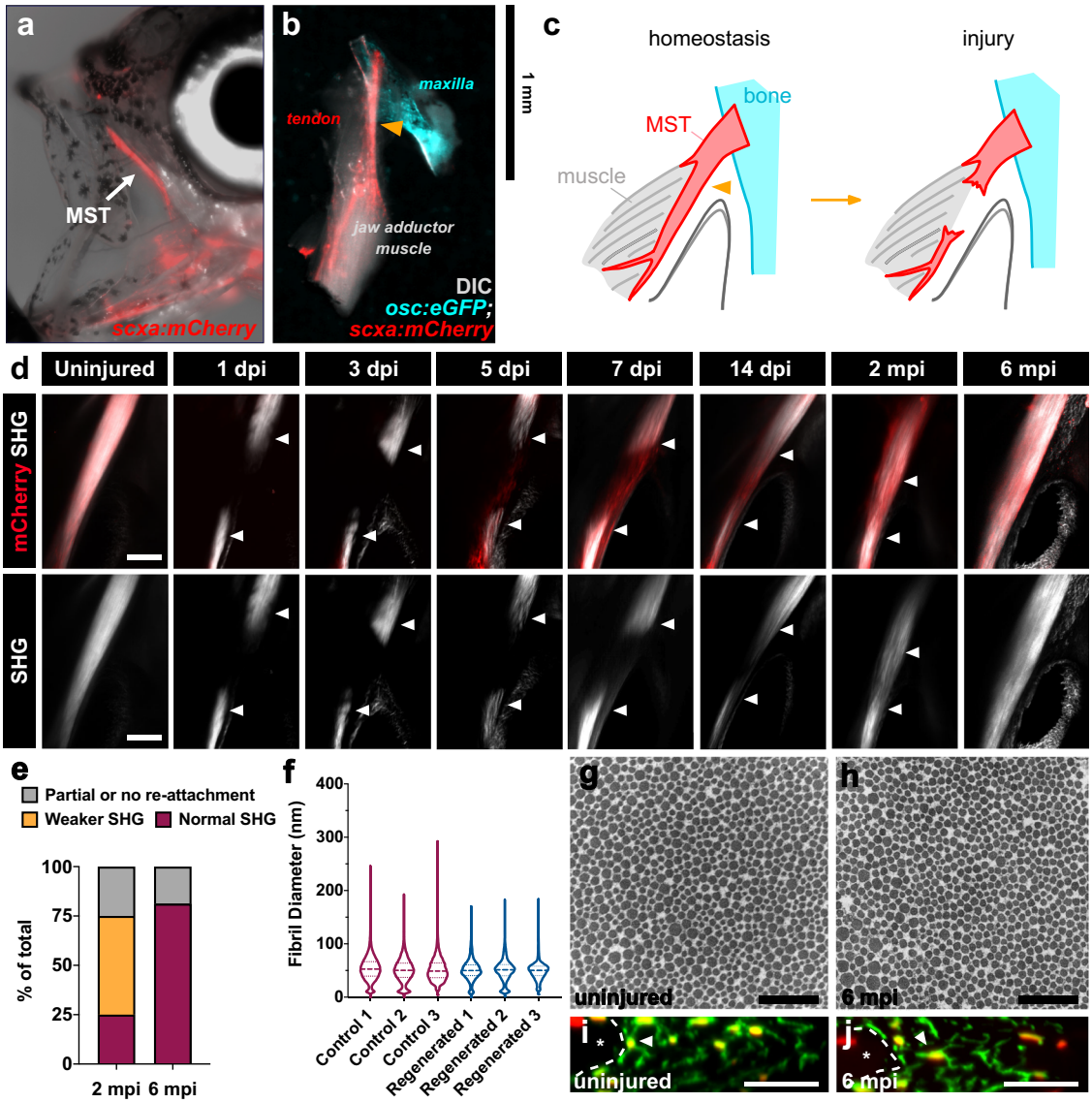

Fig. 1 The adult zebrafish can fully regenerate after acute injury. a Epifluorescence image of an adult *scxa:mCherry* zebrafish with a brightfield overlay to demonstrate the position of the maxillary superficial tendon (MST) (denoted by white arrow). **b** Epifluorescence image of a normal uninjured MST musculoskeletal circuit (i.e. maxilla, MST, jaw adductor muscle (A0)) dissected from an *osc:eGFP;scxa:mCherry* adult zebrafish with a DIC overlay. The Orange arrowhead denotes where the injury is made. **c** Graphical schematic of the MST before and after injury. **d** 2-photon images of the MST at various time points after injury in *scxa:mCherry* zebrafish with SHG signal both overlaid and shown separately. White arrowheads denote the severed tendon ends. Scale bar, 100 µm. **e** Stacked bar graph showing the breakdown of zebrafish exhibiting partial or no reattachment, weaker SHG signal, or fully restored SHG signal at 2- and 6-months post-injury (mpi) (2 mpi: $N = 12$; 6 mpi: $N = 16$). **f** Violin plot illustrating the collagen fibril diameter distribution in 3 age-matched individuals uninjured and regenerated MSTs at 6 mpi. The means of uninjured controls 1, 2, and 3 were 53.33, 50.24, and 51.35 nm, respectively. Means of injured MSTs 1, 2, and 3 were 50.62, 50.31, and 49.41 nm respectively. Quartile values are shown with a dotted line and the median is shown with a dashed line. **g**, **h** Representative 50,000x TEM micrographs from age-matched uninjured (**g**) and regenerated tendons at 6 mpi (**h**). Scale bar, 500 nm. **i**, **j** Representative images of a cross-sectional re-slice view of 2-photon *z*-stacks from anti-mCherry stained (shown in green) *scxa:mCherry* MSTs from age-matched control uninjured (**i**) and regenerated MSTs at 6 mpi (**j**). White dotted lines outline muscle boundaries and asterisks mark muscles. Scale bar, 10 µm.

tendon (MST) in *scxa:mCherry* zebrafish and monitored the recovery (Fig. 1a–d). The MST connects the maxilla to one of the jaw adductor muscles, specifically classified as the A0 adductor muscle (Fig. 1a–b)[18,19]. The midbody of the MST contains a short segment with only midbody tenocytes and a longer segment that runs along the adductor muscle and contains a mixture of both MTJ cells and midbody tenocytes. In the latter region, all cells express the tendon marker *tnmd*, and cells only in direct contact with the muscle express the myotendinous marker *col22a1* (Fig. 1c, Supplementary Fig. 1)[20–23]. For technical reproducibility, we chose to perform a full transection of the tendon at its midpoint towards the beginning of the longer segment. We also strategically chose the MST because its superficial nature makes it ideal for experimental use as it is easy to access, surgically manipulate, and image. In addition, while it functions in closing the mouth[19], it is not required for feeding, allowing fish to eat normally and survive following surgery.

We performed 2-photon imaging at different time points post-injury to monitor the recovery, which allowed us to simultaneously visualize *scxa:mCherry* expression and second harmonic generation

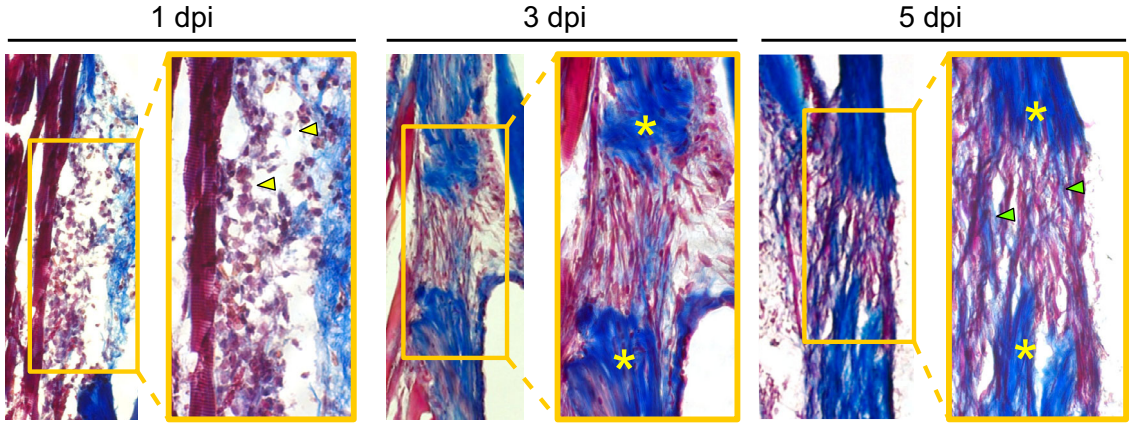

Fig. 2 Tendon regeneration proceeds through a rapid series of phases within the first week post-injury. Masson's trichrome staining of sections from regenerating tendons at 1 (left), 3 (middle), and 5 (right) dpi. Heavy infiltration of cells with myeloid-like morphologies can be seen at 1 dpi (yellow arrowheads). At 3 dpi, a fibroblastic bridge connecting the two severed tendon ends is evident. By as early as 5 dpi, the beginnings of collagen matrix deposition into the injury site are observed (green arrowheads). Yellow asterisks denote severed tendon ends and images were taken at 10x magnification. Dpi, days post-injury.

(SHG) signal to assess collagen fiber alignment (Fig. 1d). The uninjured tendon exhibits both strong *scxa:mCherry* expression and SHG signal as expected. At 1 and 3 days post-injury (dpi), there is a loss of *scxa:mCherry* expression and SHG signal at the injury site. However by 5 and 7 dpi, a *scxa:mCherry+* bridge between the severed tendon ends can be observed and appears to become more organized by 14 dpi. In addition, we examined the expression of another connective tissue marker *periostin b* (*postnb*) which is highly expressed in the tendon using an existing *postnb:citrine* reporter line[24] (Supplementary Fig. 2). We observed strong ubiquitous *postnb:citrine* expression in the uninjured tendon as well as in various surrounding interstitial connective tissues and the periosteum. At 4 dpi, we observed *postnb:citrine+* cells within a subset of cells in the bridging tissue in a largely overlapping domain with *scxa:mCherry* expression. By 14 dpi, both *postnb:citrine* and *scxa:mCherry* are strongly expressed throughout the entire cellular bridge, suggesting that tendon gene expression programs may be downregulated upon injury.

By 2 months post-injury (mpi), SHG signal begins to return at the injury site and appears to be fully restored by 6 mpi. When we examined the qualitative breakdown of SHG signal restoration following injury, we observed that 25% of injured fish ($N = 3/12$) had fully restored SHG signal at the injury site at 2 mpi whereas 50% ($N = 6/12$) displayed weaker SHG signal (Fig. 1e). By 6 mpi, 81.25% of injured fish ($N = 13/16$) exhibited a full restoration of SHG signal, indicating collagen fiber alignment in the tendon matrix had returned. We also observed that some fish exhibited partial or no re-attachment of the severed tendon ends ($N = 3/16$), leading to a complete failure of SHG signal restoration.

We next sought to examine whether the collagen matrix ultrastructure and tenocyte morphology/network regenerated following injury. To assess if the collagen fibril diameter distribution was re-established, we performed transmission electron microscopy (TEM) of control and injured tendons at 6 mpi (Fig. 1f–h). We observed no significant difference in collagen fibril diameter distributions between control and injured tendons at 6 mpi, suggesting that the collagen matrix was fully restored. Furthermore, tenocytes in the injury site reassumed a normal elongated tenocyte morphology with thin processes extending between neighboring cells, indicating the tenocyte network is re-established in injured tendons by 6 mpi (Fig. 1i, j). Altogether, these data strongly show that the adult zebrafish tendon fully regenerates following acute injury, unlike their mammalian counterparts.

Tendon injury triggers a swift innate immune response, cellular proliferation, and collagen fiber deposition during the first week post-injury

As the formation of an organized *Scx+* cellular bridge does not occur following full transection in mammalian tendons[12], we sought to better characterize early events during zebrafish regeneration. Masson's trichrome staining of the regenerating tendon at 1, 3, and 5 dpi revealed a rapid sequence of events surrounding bridge formation during the first week post-injury. At 1 dpi, there is a heavy infiltration of cells, many of which exhibit monocytic and granulocytic morphologies (e.g. rounded, large multi-lobed nuclei), suggesting the onset of an innate immune response. By 3 dpi, a cellular bridge has begun to form between the two severed tendon ends containing cells that exhibit fibroblastic morphologies. At 5 dpi, the beginnings of collagen deposition are evident as seen by the presence of collagen fibers stained in blue (Fig. 2).

To examine innate immune cell dynamics during tendon regeneration in more depth, we performed time course 2-photon imaging of *Tg(mpx:eGFP)* and *Tg(mpeg:eGFP)* lines to examine neutrophil and macrophage infiltration, respectively (Fig. 3a, b). Overall, both cell types demonstrated significant dynamic changes in infiltration that were relatively similar after injury (****$p < 0.0001$, one-way ANOVA). We observed little to no neutrophils or macrophages in the homeostatic tendon at 0 dpi. However, by 12 h post-injury (hpi), there was a rapid and significant increase in both cell types at the site of injury (*mpx+* cells: 0.21% (0 dpi) vs. 15.09% (12 hpi), ****$p < 0.0001$, *mpeg+* cells: 0.0% (0 dpi) vs. 11.78% (12 hpi), ****$p < 0.0001$). By 1 dpi, the percentage of neutrophils in the injury site significantly decreased (15.09% (12 hpi) vs. 6.34% (1 dpi), ****$p < 0.0001$) whereas the percentage of macrophages did not significantly change from 12 hpi. However, the percentage of both immune cell types continued to decrease over time from 1 to 5 dpi, at which point near basal levels were reached (*mpx+* cells: 6.34% (1 dpi) vs. 0.91% (5 dpi), **$p < 0.01$, *mpeg+* cells: 8.20% (1 dpi) vs. 1.26% (5 dpi), *$p < 0.05$). At 14 dpi, virtually no neutrophils or macrophages remained at the injury site. These data indicate that tendon injury triggers a robust yet transient innate immune response that peaks at 12 hpi and begins to decline thereafter to basal levels at 5 dpi.

We next asked whether bridge formation coincides with a peak in cellular proliferation of a potential progenitor population that ultimately regenerates the tendon. To examine proliferating cells, we pulsed regenerating zebrafish with EdU 24 h prior to imaging to assess the percentage of proliferating cells at different time points

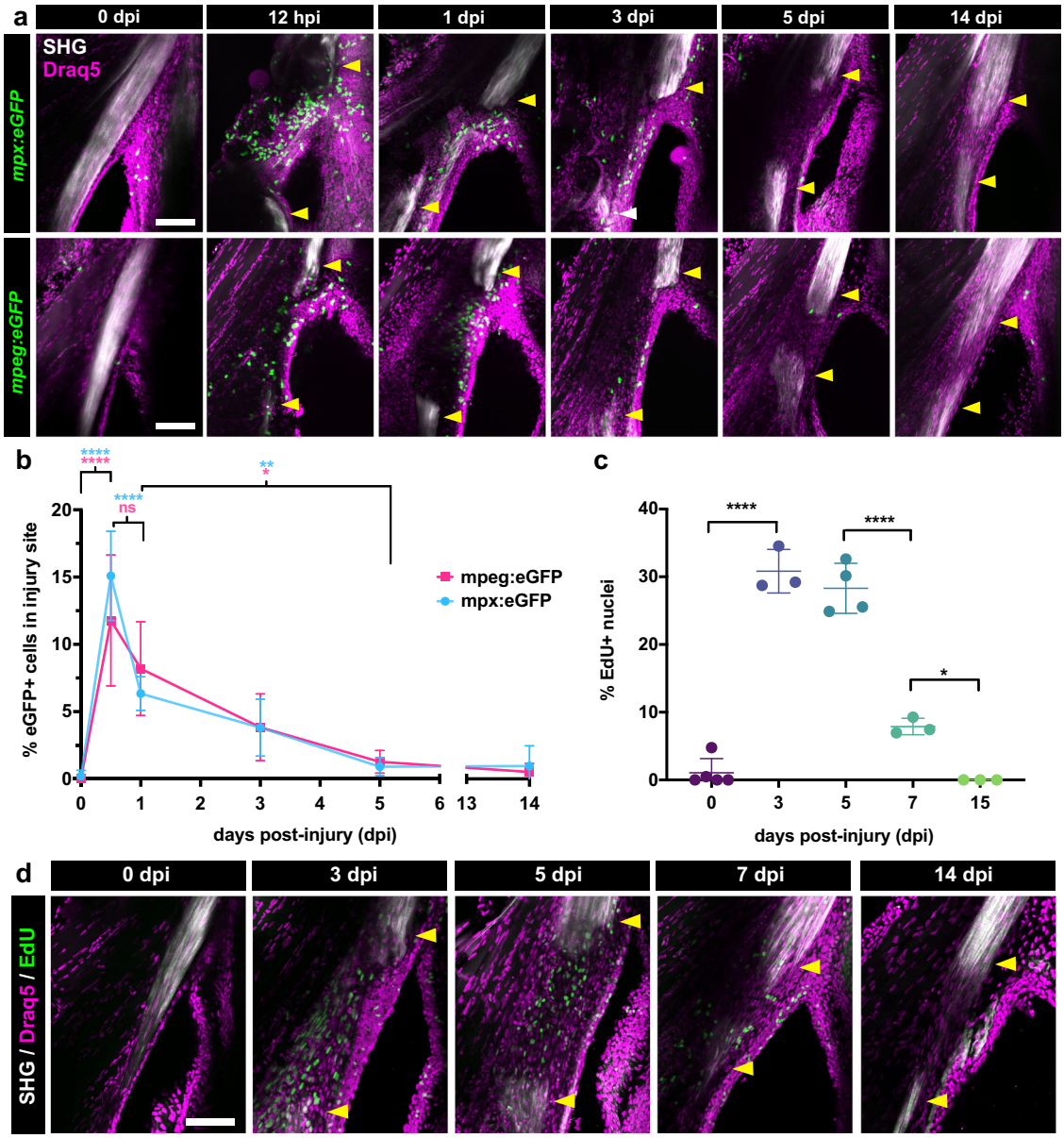

Fig. 3 Tendon injury triggers a rapid innate immune response followed by a wave of cellular proliferation. a 2-photon imaging of regenerating tendons from *mpx:eGFP* (top row) or *mpeg1:eGFP* (bottom row) zebrafish at different time points post-injury to examine neutrophil and macrophage dynamics, respectively. SHG signal is overlaid along with a Draq5 nuclear counterstain. Yellow arrowheads denote severed tendon ends. Scale bar, 100 µm. **b** Quantification of the percentage of *mpx:eGFP*+ and *mpeg1:eGFP*+ cells out of total Draq5+ cells in the injury site during the first 2 weeks post-injury. One-way ANOVA analysis was employed for statistical analysis with Tukey's multiple comparison tests between different time points. Sample sizes were as follows: *mpx:eGFP* – 0, 1, 14 dpi: $N = 4$; 0.5, 3, 5 dpi: $N = 5$; *mpeg1:eGFP* – 0.5 dpi: $N = 6$; 0, 1, 3 dpi: $N = 5$; 5 dpi: $N = 4$; 14 dpi: $N = 3$. ****$p < 0.0001$, **$p < 0.01$, *$p < 0.05$. **c** Quantification of the percentage of EdU+ cells out of total Draq5+ cells in the injured area at 0, 3, 5, 7, and 15 dpi. One-way ANOVA analysis was employed for statistical analysis with Tukey's multiple comparison tests between time points. Sample sizes were as follows: 0 dpi: $N = 5$; 3, 7, 15 dpi: $N = 3$; 5 dpi: $N = 4$. ****$p < 0.0001$, *$p < 0.05$. **d** Representative 2-photon time course imaging of EdU+ cells (in green) at different time points post-injury. SHG signal is overlaid with Draq5 nuclear staining. Yellow arrowheads denote severed tendon ends. Scale bar, 100 µm. All error bars in graphs denote the standard deviation.

post-injury (Fig. 3c, d). We observed significant changes in the percentage of EdU+ cells during the early stages of regeneration (****$p < 0.0001$, one-way ANOVA). As expected, little to no EdU+ cells were present in the uninjured tendon at 0 dpi. However, there was a statistically significant increase in the percentage of EdU+ cells at the injury site at 3 dpi (1.05% (0 dpi) vs. 30.82% (3 dpi), ****$p < 0.0001$) which was steadily maintained through 5 dpi, began to significantly decrease at 7 dpi (28.30% (5 dpi) vs. 7.88% (7 dpi),****$p < 0.0001$), and ultimately declined down to basal levels at 15 dpi (7.88% (7 dpi) vs. 0.00% (15 dpi), *$p < 0.05$). Collectively, these data indicate that tendon injury triggers a series of hallmark events within the first 5 days after injury including a strong innate immune response followed by increased cellular proliferation and the onset of collagen matrix deposition.

Endogenous tenocytes are a major cellular source of tendon regeneration

While neonatal mammalian *Scx*-lineage tendon cells can respond to injury and regenerate the Achilles tendon following full

transection, adult *Scx*+ tenocytes fail to respond upon the same injury and do not contribute to healing[12]. Therefore, we asked whether adult zebrafish tenocytes may differ from their counterparts in mice and retain the ability to respond to injury and contribute to tendon regeneration. To examine this question, we generated a *scxa:creERT2* BAC transgenic zebrafish line to perform lineage tracing of tenocytes during regeneration (Fig. 4). We first validated the specificity of the *Tg(scxa:creERT2)* line in larvae by performing both double in situ hybridization chain reaction (HCR) of *scxa/cre* and 4-hydroxy-tamoxifen (4-OHT) labeling during tendon development. HCR double in situ hybridization of *scxa* and *cre* expression in *scxa:creERT2* larvae at 4 days post-fertilization (dpf) confirmed *cre* expression in *scxa*+ craniofacial tendons and ligaments including the hyohyal (hh) and sterno-hyoidus (sh) tendons as well as the lateral ligaments (l) (Fig. 4a). Furthermore, 4-OHT induction of *scxa:creERT2;ubi:zebrabow* larvae from 48–96 h post-fertilization (hpf) efficiently and specifically labeled cells within tendons in the craniofacial region including the sh tendon as well as the myosepta in the trunk region (Fig. 4b–d). Finally, we performed 4-OHT labeling in adult *scxa:creERT2;ubi:zebrabow* zebrafish in the adult MST during homeostasis to assess the efficiency of labeling in adulthood (Fig. 4e-j). We observed labeling throughout the tendon from the tendon-bone attachment (Fig. 4g–h) to the midbody and myotendinous junction (Fig. 4i–j). Quantification of co-labeling between *scxa-lineage* tenocytes and *scxa*-expressing cells detected via RNAscope in situ hybridization revealed a labeling efficiency of approximately of 45.78% ± 3.19% (Fig. 4k). Importantly, we observed that the percentage of CFP + /YFP+ labeled tenocytes remained stable after 7 days post-induction, thus for all subsequent adult lineage tracing experiments we chose to perform the injuries at 7 days post 4OH-T administration (Supplementary Fig. 3). Altogether, these data demonstrated the specificity and utility of this transgenic line for tendon lineage tracing studies.

To determine if *scxa*+ tenocytes contribute to tendon regeneration, we induced CFP and/or YFP labeling in *scxa:creERT2;ubi:zebrabow* zebrafish through 4-OHT administration one week prior to injury and examined the contribution of *scxa*-lineage cells to the regenerating tendon at 4 and 14 dpi (Fig. 5a). At 4 dpi, we observed the presence of CFP+ and/or YFP+ *scxa*-lineage cells at the injury site that appeared to have a more rounded, less elongated morphology (Fig. 5a, b). By 14 dpi, CFP- and YFP-labeled cells re-adopted an elongated morphology at the injury site, indicating reacquisition of mature tenocyte features (Fig. 5b). Quantification of the contribution of *scxa-lineage* cells at 14 dpi showed that 55.88% ± 6.93% of cells in the regenerating bridging tissue were derived from the *scxa-lineage* (Fig. 5c). In addition, CFP and YFP-labeled cells were co-labeled with EdU in both of the severed tendon ends and at the injury site at 4 dpi (Fig. 5d–e), demonstrating that pre-existing tenocytes proliferate and migrate to the site of injury. Together, our data indicates that pre-existing tenocytes proliferate, migrate to the wound, and regenerate the tendon, collectively positioning them as the main cell source of adult zebrafish tendon regeneration.

TGF-β signaling is required for tendon regeneration

TGF-β signaling plays central roles in tendon development, maintenance, and repair, and notably, this pathway is required for mouse neonatal tendon regeneration[6,11,25]. Therefore, we sought to investigate whether TGF-β signaling is also required for adult zebrafish tendon regeneration. We first examined if TGF-β signaling is active in the uninjured and regenerating tendon by examining the expression of type I and type II TGF-β receptors *tgfbr1b and tgfbr2a* as well as a key downstream effector of canonical TGF-β signaling, p-Smad3, during homeostasis and at 4 dpi. Multiplexed RNAscope in situ hybridization of *tgfbr1b* and *tgfbr2a* in uninjured tendons revealed expression of *tgfbr1b* and little to no expression of *tgfbr2a* in *scxa*-expressing tenocytes (Fig. 6a–d). However at 4 dpi, we observed increased expression of both *tgfbr1b* and *tgfbr2a* in *scxa*-lineage tenocytes (Fig. 6e). Similarly, we observed low basal levels of p-Smad3 in tenocytes in uninjured tendons and increased p-Smad3 expression in CFP + / YFP+ *scxa*-lineage tenocytes at the injury site at 4 dpi (Fig. 6f), together demonstrating that *scxa*-lineage tenocytes are responsive to TGF-β signaling during homeostasis and regeneration. In addition, increased expression of *tgfbr1b*, *tgfbr2a*, and p-Smad3 was also observed in the surrounding tissues at the injury site indicating a general upregulation of TGF-β signaling upon injury (Fig. 6e, f).

To test whether TGF-β signaling is required for tendon regeneration, we treated regenerating zebrafish with the Alk4/5/7 inhibitor SB-431542 for the first week of regeneration beginning either immediately after injury (0 dpi) or at 1 dpi to avoid the peak of innate immune responses (Fig. 7a). As expected, SB-431542 treatment led to decreased expression of p-Smad3 after injury validating efficient TGF-β inhibition (Supplementary Fig. 4a). We observed a severe inhibition of *scxa:mCherry* bridge formation at 7 dpi in SB-431542-treated zebrafish in both experimental regimens (Fig. 7b). TGF-β-inhibited fish exhibited a significant decrease in the percentage of *scxa:mCherry*+ cells infiltrating the injury site at 7 dpi when treatment began at 0 dpi (DMSO vs. SB-43152: 75.74% ± 12.17% vs. 8.80% ± 7.02%, ****$p < 0.0001$) and 1 dpi (DMSO vs. SB-43152: 79.64% ± 3.91% vs. 10.24% ± 7.85%, ****$p < 0.0001$) (Fig. 7c). Interestingly, cell density remained unchanged at the injury site; despite a significant decrease in the *scxa:mCherry*+ cell density at the injury (Supplementary Fig. 4d–e). Furthermore, SB-431542-treated zebrafish displayed a significantly larger defect size between the two severed tendon ends at 7 dpi in both treatment regimens (DMSO vs. SB431542: 0-7 dpi, 148.4 ± 26.53 µm vs. 435.5 ± 77.75 µm; 1-7 dpi, 164.4 ± 36.00 µm vs. 401.1 ± 50.94 µm, ****$p < 0.0001$) (Fig. 7d). We also observed an expansion of cells, resembling epithelial cells, in the defect at 4 dpi in zebrafish treated from 1-4 dpi (Supplementary Fig. 4b, c). Collectively, these data highlight a requirement for TGF-β signaling in tendon regeneration.

As we observed a defect in bridge formation, we next investigated whether TGF-β signaling is required more specifically for tenocyte proliferation and/or recruitment. To this end, we first performed lineage tracing in combination with SB-431542 treatment to examine if TGF-β inhibition impaired tenocyte recruitment to the injury site (Fig. 8a). We observed a significant decrease in the percentage of *scxa*-lineage tenocytes infiltrating the injury site at 7 dpi in both treatment regimens (Fig. 8b, c) (DMSO vs. SB-431542: 0-7 dpi, 39.71% ± 7.56% vs. 13.28% ± 2.52%, ****$p < 0.0001$; 1-7 dpi, 39.11% ± 9.52% vs. 14.39% ± 6.27%, ***$p < 0.001$), indicating a severe defect in the recruitment of tenocytes. Furthermore, SB-treatment also led to a significant decrease in *scxa*-lineage cell density at the injury site (Supplementary Fig. 4f). To determine if this impairment could be a result of a diminished cell source via decreased tenocyte proliferation, we performed EdU labeling in injured fish treated with DMSO or SB-431542 from 1-4 dpi to examine the proliferation of *scxa*-lineage tenocytes (Fig. 8d, e). We observed no significant difference in EdU+ *scxa*-lineage tenocytes in the severed tendon ends at 4 dpi (Fig. 8f, g). Moreover, despite observing a significant decrease in the percentage of *scxa*-lineage tenocytes recruited to the injury site at 4 dpi (DMSO vs. SB-431542: 34.82% ± 8.91% vs. 12.51% ± 7.87%, **$p < 0.01$), there was no significant difference in the percentage that divide at the defect (Fig. 8h, i). These data therefore indicate that TGF-β signaling is required for tenocyte recruitment, but not proliferation during bridge formation in tendon regeneration.

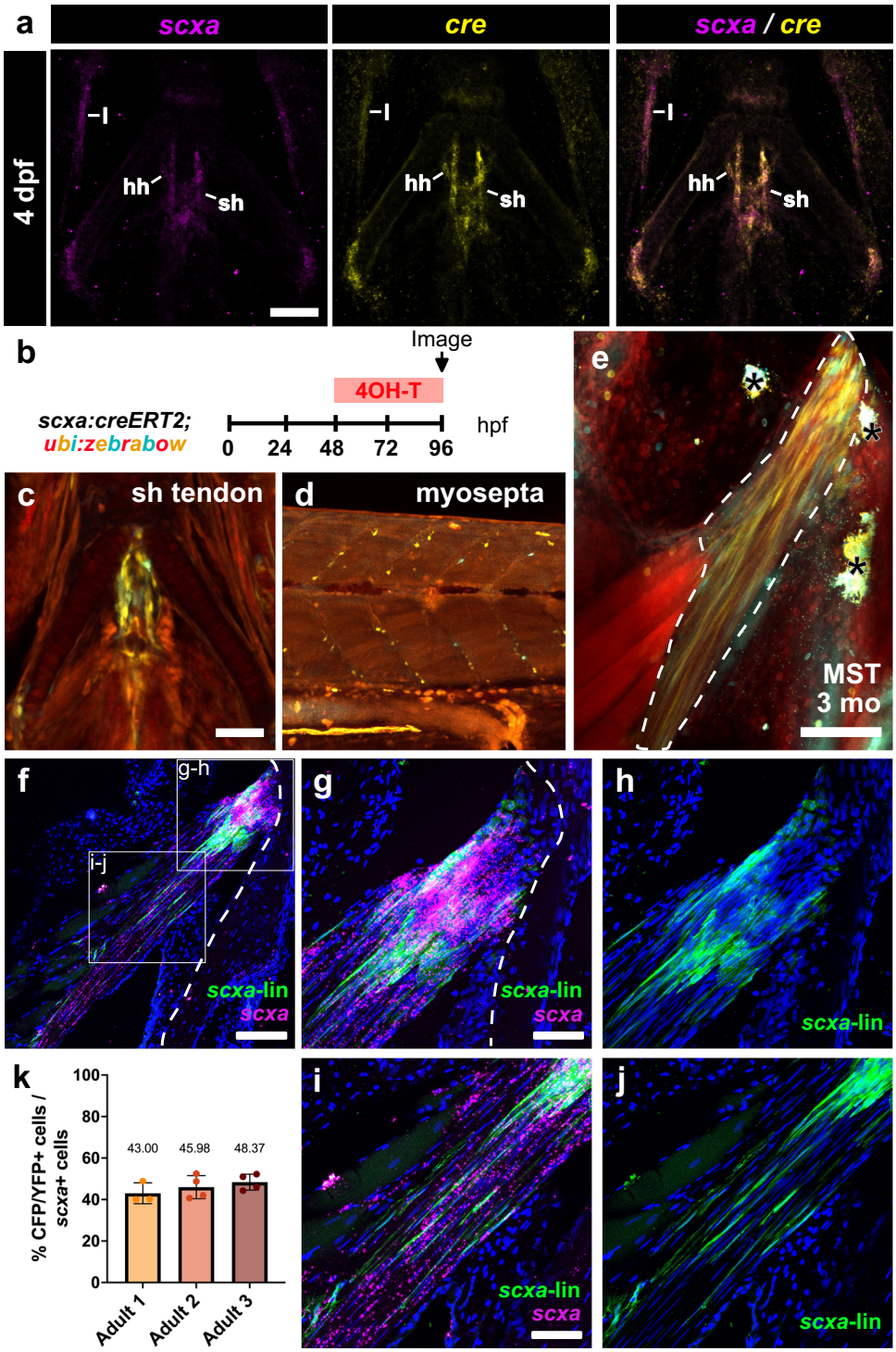

Fig. 4 Generation and validation of a *scxa:creERT2* transgenic line. a HCR double in situ hybridization of *scxa* and *cre* at 4 days post-fertilization (dpf) shows overlap in expression in craniofacial tendons and ligaments. l, lateral ligament; sh, sternohyoidus tendon; hh, hyohyal tendon. Scale bar, 50 µm. **b** Schematic of 4OH-T labeling experiment to test tendon labeling in *scxa:creERT2; ubi:zebrabow* larvae. **c**, **d** Representative confocal images from the 4OH-T labeling validation experiment in (**b**). The labeled SH tendon is shown in c and labeled myoseptal cells in the trunk region are shown in d at 96 h post-fertilization (hpf). Scale bar, 50 µm. **e** Representative 2-photon image of 4OH-T labeling in the 3-month-old adult MST (outlined in white dotted line). Asterisks denote autofluorescent pigment in the skin. Scale bar, 100 µm. **f** Confocal image of anti-GFP immunofluorescence to detect CFP+ and/or YFP+ *scxa*-lineage cells (green) combined with RNAscope in situ hybridization of *scxa* (magenta). Scale bar, 100 µm. **g**, **h** Higher magnification (40x) confocal image of the tendon-bone attachment region of the MST from panel f. *scxa*-lineage cells overlayed with *scxa* signal are shown in g, while *scxa*-lineage cells are shown in h. Scale bar, 50 µm. **i**, **j** Higher magnification (40x) confocal image of the midbody region of the MST from panel (**f**). *scxa*-lineage cells overlayed with *scxa* signal are shown in (**i**), while *scxa*-lineage cells are shown in (**j**). Scale bar, 50 µm. **k** Quantification of the efficiency of *scxa:creERT2* labeling in 3 independent adult zebrafish (measuring the percentage of CFP+ and/or YFP+ cells (in green) out of total *scxa*-expressing cells (in magenta) as detected by RNAscope in situ hybridization). Means of quantified sections from each fish are listed above and error bars in the bar graph denote the standard deviation.

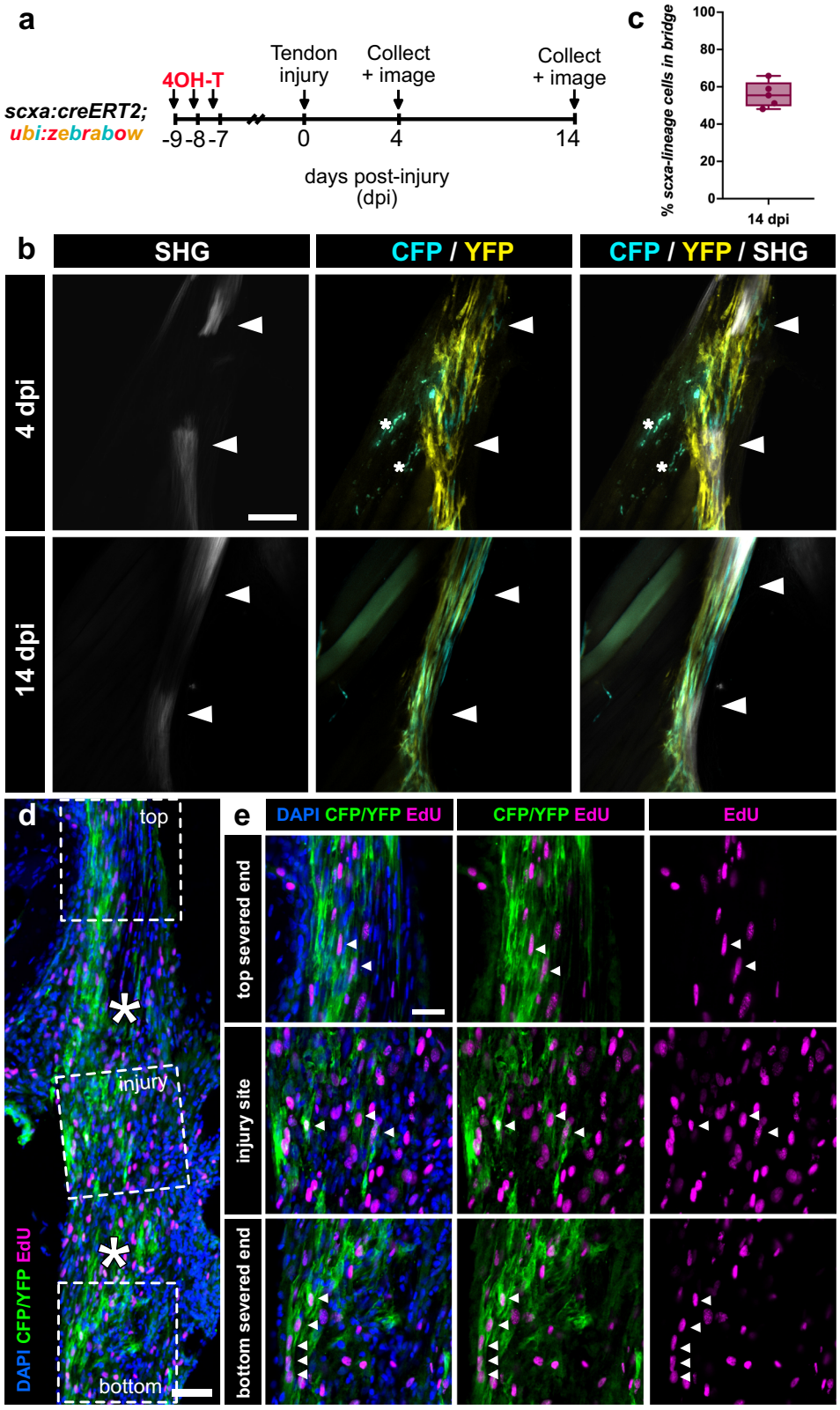

DISCUSSION

Our study sets the groundwork for utilizing the adult zebrafish tendon as a means for uncovering molecular mechanisms required for proper regeneration. We demonstrate that the adult zebrafish tendon can regenerate following an acute full transection injury and identify endogenous tenocytes as the main cellular source of regeneration. Tendon regeneration progresses through three main phases: inflammation, tendon bridge formation via tenocyte proliferation and migration, and re-differentiation/maturation coupled with matrix remodeling (Fig. 9). These

Fig. 5 Pre-existing tenocytes are a major cell source of tendon regeneration. a Experimental schematic of *scxa:creERT2; zebrabow* lineage tracing experiment during tendon regeneration. **b** 2-photon imaging showing CFP+ and/or YFP+ *scxa*-lineage cells infiltrating the injury site at both 4 and 14 days post-injury (dpi). SHG signal is shown either separately or overlaid. White arrowheads denote severed tendon ends. Asterisks denote autofluorescent blood cells. Scale bar, 100 µm. **c** Quantification of the percentage of CFP+ and/or YFP+ *scxa*-lineage cells in the regenerating tendon bridge between the severed tendon ends at 14 dpi ($N = 5$, mean percentage = 55.88% ± 6.93%). The box and whiskers plot shows whiskers extending from the minimum to maximum values, a line at the median, and a box encompassing the 25th to 75th percentiles. **d** Representative confocal image of an anti-CFP/YFP stained (in green) section of a regenerating tendon at 4 dpi coupled with EdU labeling (in magenta). Higher magnification of regions of the top severed end, injury site, and bottom severed end are shown in e. Asterisks denote the severed tendon ends. Scale bar, 25 µm. **e** Higher magnification confocal imaging of CFP/YFP stained cells co-labeled with EdU in the top and bottom severed tendon ends as well as the site of injury. White arrowheads denote examples of CFP/YFP+ cells co-labeled with EdU. Scale bar, 25 µm.

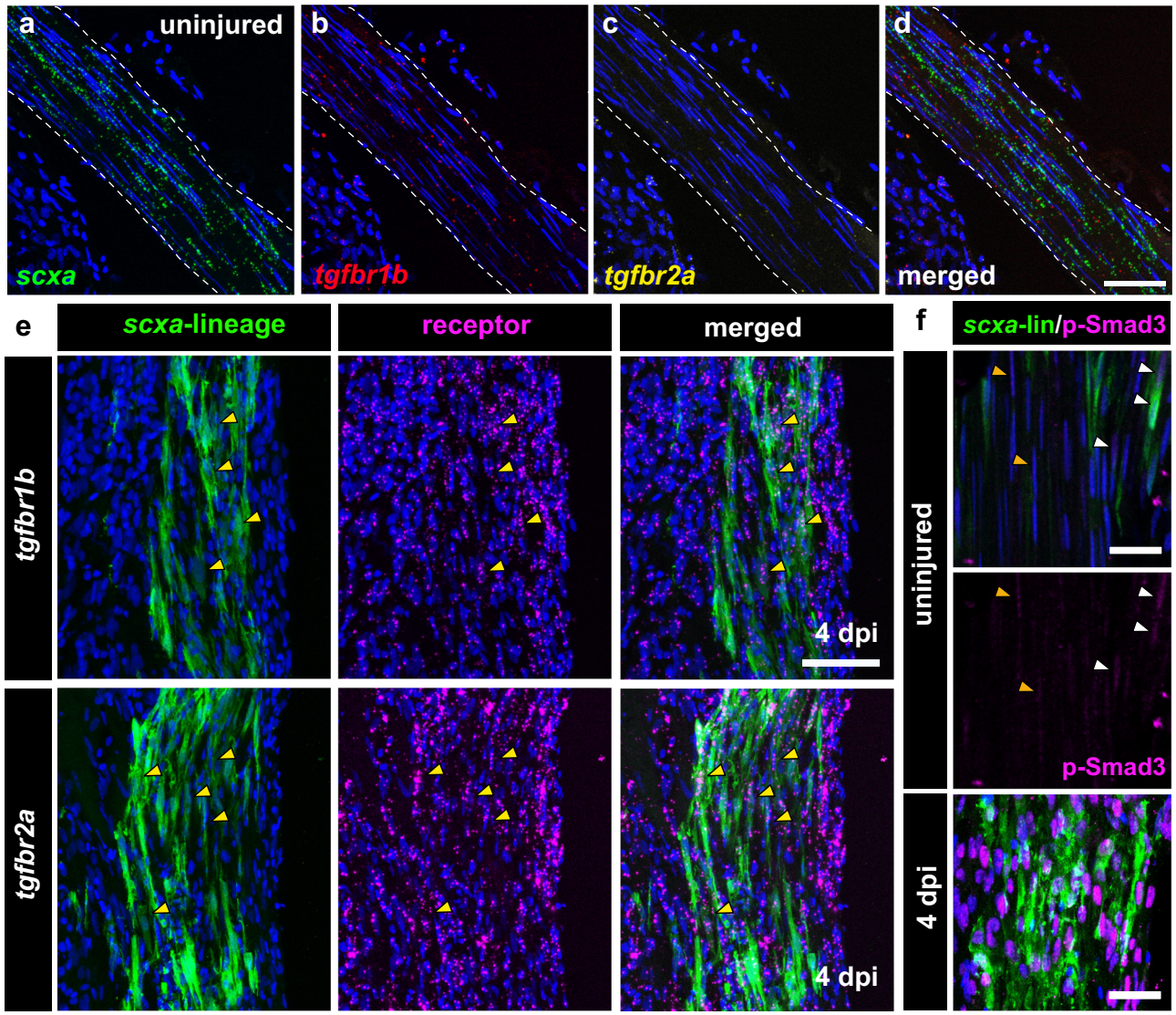

Fig. 6 TGF-β signaling is active in tenocytes during regeneration. a–d Multiplexed RNA-scope in situ hybridization of *scxa* (green, **a**), *tgfbr1b* (red, **b**), and *tgfbr2a* (yellow, **c**) in the uninjured tendon. The merged image of all three is shown in (**d**). Scale bar, 50 µm. **e** Confocal images of anti-GFP immunofluorescence to detect CFP+ and/or YFP+ *scxa*-lineage cells (in green) combined with RNAscope in situ hybridization of either *tgfbr1b* (top panels) or *tgfbr2a* (bottom panels) in magenta at 4 days post-injury (dpi). Yellow arrowheads denote examples of co-positive cells. Scale bar, 50 µm. **f** Double immunostaining of anti-GFP immunofluorescence to detect CFP+ and/or YFP+ *scxa*-lineage cells (in green) with p-Smad3 staining (in magenta) in uninjured and regenerating tendons at 4 dpi. The middle panel shows the p-Smad3 staining alone in the uninjured tendon split from the merged image in the top panel. Orange and yellow arrowheads denote weakly p-Smad3+ nuclei in unlabeled and labeled tenocytes from lineage tracing, respectively. Scale bars, 25 µm.

stages advance in a semi-overlapping sequence within the first week post-injury, with the exception of tenocyte differentiation/maturation and matrix remodeling which spans up to 6 mpi, altogether demonstrating the immense time required to rebuild the distinct collagen matrix ultrastructure.

The inherent regenerative capability of the adult zebrafish tendon may be directly linked to the ability of their tenocytes to proliferate and migrate to the site of injury, forming a regenerative bridging tissue between the two severed tendon ends. Adult mammalian tenocytes appear to lack this ability as it has been

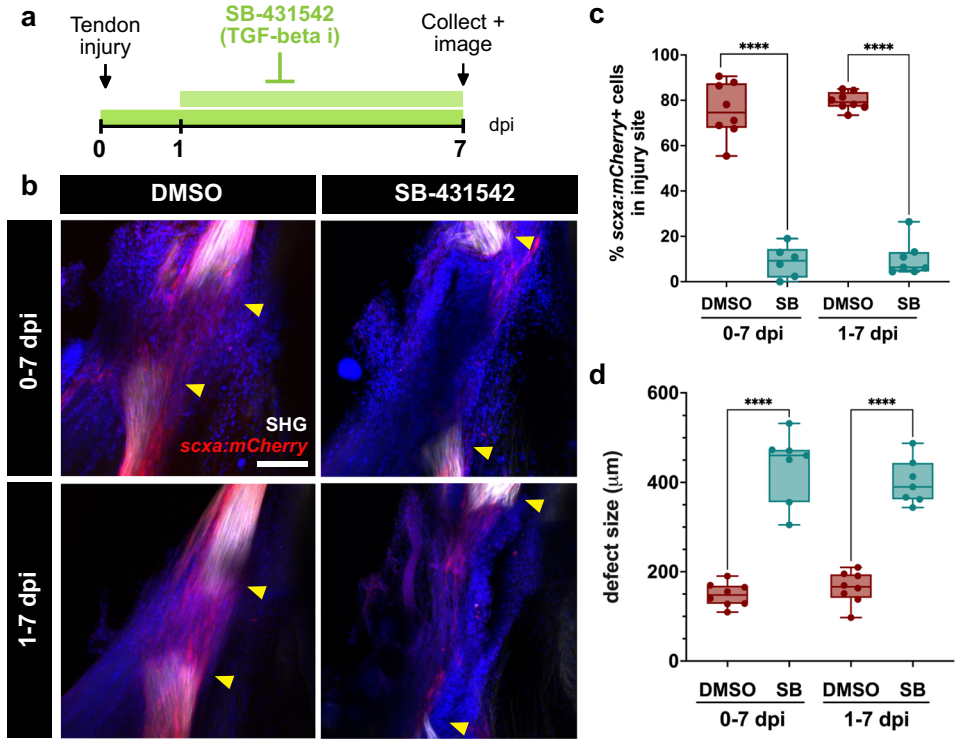

Fig. 7 Canonical TGF-β signaling is required for adult zebrafish tendon regeneration. a Schematic of experimental design for inhibition of TGF-β signaling during tendon regeneration. **b** Representative 2-photon stacks of DMSO and SB-431542-treated regenerating tendons at 7 days post-injury (dpi) in *scxa:mCherry* zebrafish overlaid with second harmonic generation (SHG) signal and Draq5 (in blue) to label nuclei. The 0-7 dpi treatment and 1-7 dpi treatment are shown in the top and bottom panels, respectively. Yellow arrowheads denote the severed tendon ends. Scale bar, 100 µm. **c** Quantification of the percentage of *scxa:mCherry*+ cells detected in the injury site at 7 dpi in DMSO and SB-431542-treated zebrafish for both the 0-7 dpi and 1-7 dpi treatments. Unpaired two-tailed *t*-tests comparing DMSO controls for each treatment with their respective SB-431542-treated counterparts were performed for statistical analysis (0-7 dpi: DMSO, $N = 8$; SB, $N = 6$; 1-7 dpi: DMSO, $N = 8$; SB, $N = 7$). ****$p < 0.0001$. **d** Quantification of the defect size at 7 dpi in DMSO and SB-431542 (SB)-treated zebrafish in both the 0-7 dpi and 1-7 dpi treatments. Unpaired two-tailed *t*-tests comparing DMSO controls for each treatment with their respective SB-431542-treated counterparts were performed for statistical analysis (0-7 dpi: DMSO, $N = 8$; SB, $N = 7$; 1-7 dpi: DMSO, $N = 8$; SB, $N = 7$). ****$p < 0.0001$. Box and whiskers plots in c and d show whiskers extending from the minimum to maximum values, a line at the median, and a box encompassing the 25th to 75th percentiles.

shown that following full transection of the mouse Achilles tendon, *Scx*+ tenocytes in the severed ends incorporate EdU similar to our observations, but fail to infiltrate the site of injury[12]. Instead, the authors observed the recruitment and persistence of αSMA-expressing cells, which eventually led to the formation of fibrotic scar tissue. With this context in mind, our work pinpoints clear differences in cellular and molecular mechanisms leading to tendon regeneration in the zebrafish and fibrotic healing in adult mice following acute injuries. Foremost, it positions the adult zebrafish tendon as an informative comparative model system to elucidate both instructive and inhibitory cues required for driving the initiation of tenocyte activation in regeneration and lack thereof in mice.

While our work identifies the cellular basis of tendon regeneration in the adult zebrafish, many questions remain as to the extent of tenocyte plasticity during regeneration. We show that the tenocyte bridge begins to form by as early as 3 dpi and is initially *scxa:mCherry*-negative, but gradually gains *scxa:mCherry* expression over time. By 7 dpi, the tenocyte bridge is largely *scxa:mCherry*+. Similarly, *postnb:citrine* expression also seems to increase over time in the cellular bridge from 4 to 14 dpi, suggesting a loss and re-acquisition of tendon marker expression. Labeled tenocytes and/or their descendants which proliferate and migrate to the injury site at 4 dpi are more rounded and eventually re-adopt an elongated morphology, a key characteristic associated with tenocyte maturation, during later stages. One interpretation of these pieces of evidence suggests that tenocytes revert to a more immature cell state during the initial stages of regeneration. However, whether they dedifferentiate to a multipotent progenitor that can give rise to other connective tissues including cartilage, or to a lineage-restricted tendon progenitor remains to be determined.

Differentiating between these possibilities will likely require a deeper understanding of gene regulatory networks (GRNs) regulating tendon progenitor specification, as *Scx* remains the earliest reported tendon marker[26,27]. Tendons in the craniofacial region like the MST are derived from cranial neural crest cells (CNCCs), while those in limbs are derived from the lateral plate mesoderm[25,28,29]. Regional differences in the GRNs underlying tendon development and regeneration are therefore likely to exist and have yet to be fully explored. Whether the distinct developmental origins may influence the mechanisms driving regeneration and/or overall regenerative capacity remains an open and interesting question. Future comparative studies examining the regenerative ability across non-craniofacial tendons in zebrafish will be instrumental in extracting basic molecular principles that are commonly required for tendon regeneration regardless of differences in anatomical location or developmental origin. It is also unknown if there are changes in tendon regenerative abilities as the fish age. Although we did not observe obvious differences in regeneration between age groups, we would need to expand our sample size to adequately compare regeneration in adult and aged fish. Notably, deciphering how precise tendon lineage specification and maintenance is ensured

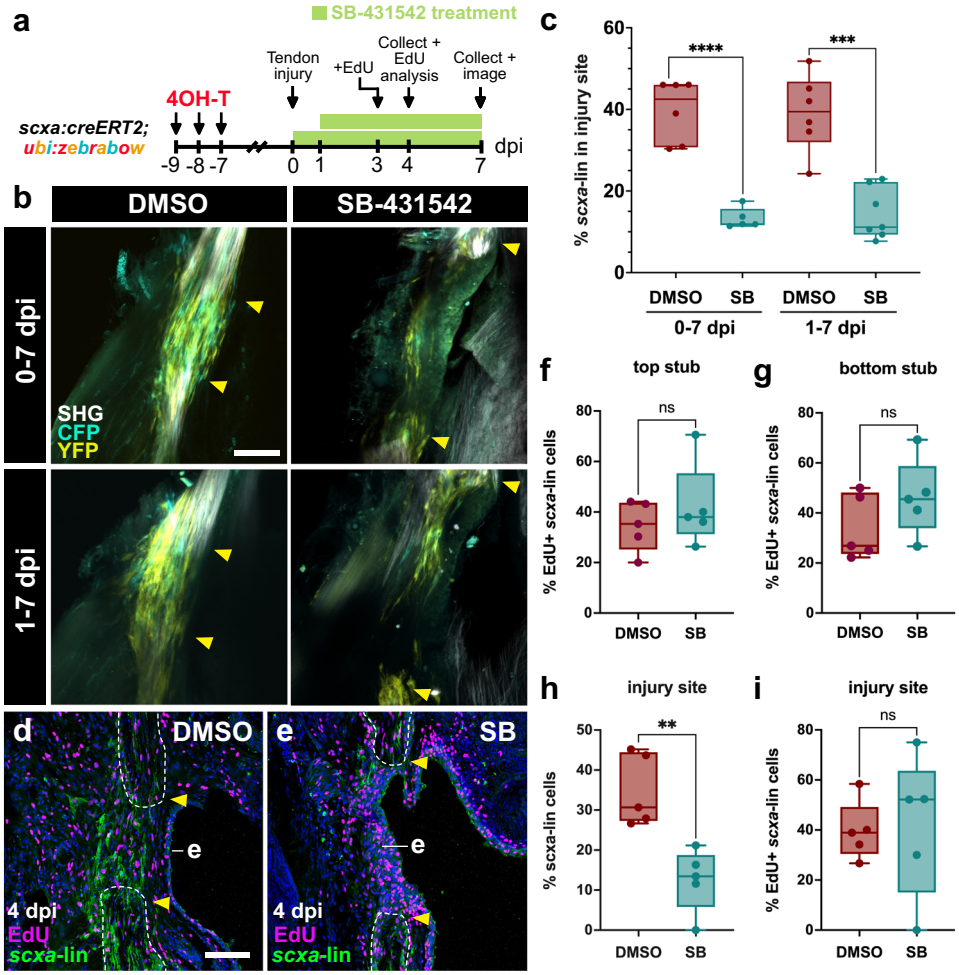

Fig. 8 TGF-β signaling is required for tenocyte recruitment, but not proliferation, during bridge formation. a Experimental schematic of combined tenocyte lineage tracing with SB-431542 treatment and subsequent analyses performed. EdU analysis was only performed on the 1-4 dpi treatment regimen. **b** 2-photon stacks of CFP+ and/or YFP+ labeled lineage-traced tenocytes in regenerating tendons at 7 days post-injury (dpi) for both 0-7 dpi and 1-7 dpi DMSO/SB-431542 (SB) treatments. Yellow arrowheads denote severed tendon ends. Scale bar, 100 µm. **c** Quantification of the percentage of *scxa*-lineage cells in the injury site at 7 dpi for both 0-7 dpi and 1-7 dpi DMSO/SB-431542 (SB) treatments. Unpaired two-tailed *t*-tests were performed between DMSO controls and their respective SB-431542 counterparts for statistical analysis (0-7 dpi: DMSO, $N = 6$; SB, $N = 5$; 1-7 dpi: DMSO, $N = 6$; SB, $N = 7$). ****$p < 0.0001$, ***$p < 0.001$. **d**, **e** Representative confocal images of EdU-stained DMSO and SB-431542 (SB)-treated regenerating tendons at 4 dpi following a 1-4 dpi treatment regimen. EdU staining is shown in magenta and anti-GFP immunofluorescence detection of *scxa*-lineage cells is shown in green. Severed tendon stubs are outlined in white dotted lines and the tendon ends are denoted by yellow arrowheads. (**e**), epidermis. **f**–**g** Quantification of the percentage of proliferating EdU+ *scxa*-lineage tenocytes in the top (**f**) and bottom (**g**) tendon ends at 4 dpi after a 1-4 dpi DMSO or SB-431542 treatment. Unpaired two-tailed *t*-tests were performed between DMSO and SB-431542 treatment conditions. ns, not significant. **h**, **i** Quantification of the percentage of *scxa*-lineage cells (**h**) and the percentage of proliferating EdU+ *scxa*-lineage tenocytes (**i**) in the injury site at 4 dpi following a 1-4 dpi SB-431542 treatment regimen. Unpaired two-tailed *t*-tests were performed between DMSO and SB-431542 treatment conditions. **$p < 0.01$; ns not significant. Box and whiskers plots in panels (**c**) and (**f**–**i**) show whiskers extending from the minimum to maximum values, a line at the median, and a box encompassing the 25th to 75th percentiles.

upon injury, regeneration, and aging can provide insight into targetable mechanisms that may be exploited clinically to prevent heterotopic ossification of tenocytes, which commonly occurs after mammalian tendon injury and compromises tissue function[30].

Nevertheless, our data raises the possibility that adult zebrafish tenocytes exhibit cellular plasticity that is more akin to fetal or neonatal tenocytes in mice. Similar to neonatal tendon regeneration[11], we identify canonical TGF-β signaling as an essential pathway that is also distinctly required for tenocyte recruitment, but not proliferation, in an adult tendon regenerative context. This strong parallel suggests that zebrafish tenocytes likely retain an intrinsic regenerative potential in adulthood that resembles that of neonatal mice. Furthermore, these findings highlight a conserved requirement for TGF-β signaling in tendon regeneration, specifically in the recruitment of *scxa/Scx*-lineage cells to the injury site, across ages (neonatal to adult) and cross-species (zebrafish and mice). Exploring if other pathways required for tendon regeneration in larval/neonatal stages including BMP[14] are also necessary in the adult will help delineate distinct and conserved requirements across ages and examine if this is unique to TGF-β signaling. In addition, it remains unclear whether all *scxa*+ tenocytes in the adult zebrafish tendon are equally competent to respond to injury. It is possible that specific subpopulations of tenocytes are more (or less) poised to respond to injury and regenerate the tendon. In mammals, several adult tendon stem/progenitor populations have been identified in vivo which contribute to tendon healing[31–35]. Elucidating whether the zebrafish tendon contains similar subpopulations and pinpointing mechanisms that may lead to differential responses during regeneration versus fibrosis will be

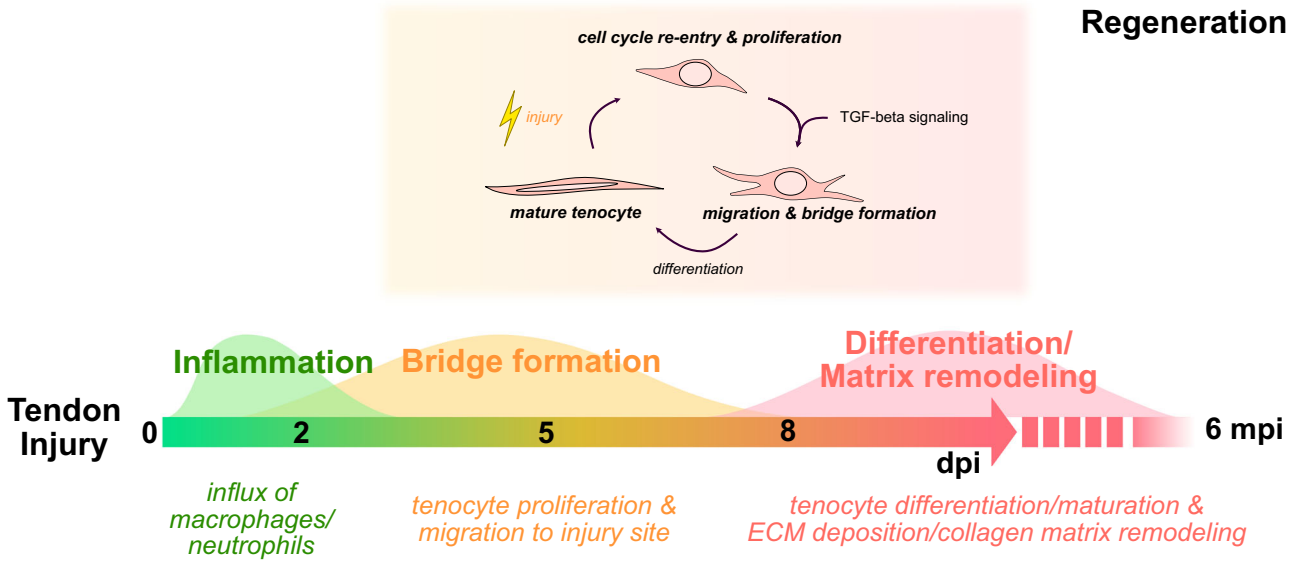

Fig. 9 Hallmarks of adult zebrafish tendon regeneration. Schematic detailing the timeline of key cellular processes following acute tendon injury and regeneration as well as the requirement of TGF-β signaling for tenocyte recruitment. dpi days post-injury, mpi months post-injury.

important next steps toward understanding the pathways and cell types that are advantageous or refractory for regeneration.

We show that TGF-β signaling is active in *scxa*+ tenocytes and is required for tenocyte recruitment to the injury site, suggesting a direct and beneficial function for TGF-β signaling in tendon regeneration. However, it is likely that TGF-β has multiple functions throughout the regenerative process and in different tendon healing contexts. TGF-β signaling is widely considered a key driver of scarring and tendon fibrosis[7,36]. Others have shown that TGF-β1 elicits divergent downstream responses which may underlie improved tendon healing in Murphy Roth's Large (MRL) mice vs. scarring in wildtype C57Bl/6 J mice[36,37]. As adult zebrafish tenocytes are TGF-β responsive during homeostasis and regeneration, it is possible that they may intrinsically respond differently to external TGF-β signaling upon injury than their adult mammalian counterparts.

Beyond its widespread roles in tendon development, maintenance, and repair[7,38–42], TGF-β signaling has a variety of functions in wound healing and inflammation[36,43,44]. We observe a general increase in both TGF-β receptor and p-Smad3 expression in the surrounding tissues as well as tenocytes after injury. Therefore, it is likely that TGF-β signaling may act on tenocytes both directly and indirectly through other surrounding TGF-β responsive cell types. Interestingly, we observed a significant expansion of cells into the defect where the tenocyte bridge normally forms with SB-431542 treatment. Based on morphology and anatomical location, we believe these cells are derived from the adjacent overlying epithelial layer, but lineage tracing experiments would be necessary to establish their origins. Finer cell-type specific genetic manipulations of TGF-β signaling will also be required in the future to determine if the expansion of these non-*scxa*-lineage cells into the injury site results directly from TGF-β inhibition or indirectly from the lack of bridge formation. It will also be interesting to explore if and how the tenocyte response is altered by the expansion of these cells into the injury site. Although we show widespread expression of TGF-β receptors, we do not know the source of the TGF-β signal. It is possible that multiple cell types within, as was shown for neonatal mouse tendons[11], and surrounding the tendon secrete TGF-β ligands. In addition, the neighboring muscle and interstitial connective tissues may also contribute and/or play a role in TGF-β signaling as well as other regenerative processes. For instance, one possibility is that muscle may be required for tenocyte differentiation and matrix maturation during regeneration similar to its role in development[15,41,45,46]. While the interactions of muscle and tendon are more well studied, our molecular understanding of the surrounding interstitial tissues is currently limited. Deeper characterization of the MST and its neighboring tissues using single cell -omics approaches will facilitate the development of new genetic tools to answer these outstanding questions.

In all, our work debuts the adult zebrafish as a powerful genetic model that can be utilized to construct a blueprint of molecular and cellular mechanisms required for proper tendon regeneration. In combination with existing mammalian tendon healing models, our findings open up an invaluable opportunity to utilize comparative cross-species genomics approaches to enable the identification of genetic regulatory and signaling dynamics essential for driving regeneration versus fibrotic healing. Identifying these mechanisms will aid in accelerating the innovation of effective tendon injury treatments in the clinic.

METHODS

Animal husbandry and zebrafish lines

All zebrafish were housed and maintained according to the MGH Institute for Animal Care and Use Committee (IACUC) protocol guidelines (Protocol #: 2012N000167). For the experimental data generated in this study, we utilized the following zebrafish transgenic lines: *TgBAC(scxa:mcherry)*[47], *Tg(mpx:eGFP)*[48], *Tg(mpeg:eGFP)*[49], *Tg(postnb:citrine)*[24], *Tg(ubi:zebrabow)*[50], *and TgBAC(scxa:creERT2)*.

Tendon injuries and chemical treatments

All zebrafish procedures were approved by MGH and performed according to MGH IACUC protocol guidelines (Protocol #: 2012N000167). Adult zebrafish from 6–15 months old were utilized for the study. To perform adult tendon injuries, zebrafish were anesthetized in 0.015% tricaine and gently pinned down with staples onto an agarose plate on their side to immobilize them. Using a small pair of dissecting scissors, the craniofacial maxillary superficial tendon (MST) was fully transected at its midpoint. The zebrafish was then returned to normal system water and monitored daily for recovery. No analgesic was used. For sample collection, zebrafish were euthanized at the indicated time points for each experiment via prolonged tricaine immersion

for at least 30 min (300 mg/L) followed by decapitation. The heads were collected and fixed in 4% paraformaldehyde overnight followed by dissection the next day to collect the MST. Depending on the experiment, MST tissue was then processed differently (see below methods). For SB-431542 treatments, MST injuries were performed on adult zebrafish as detailed above and the fish were immersed in 15 uM SB-431542 (diluted in zebrafish system water, 100 mL/fish) either immediately after injury (0 dpi) or at 1 dpi. SB-431542 solution was changed daily and fish were fed daily throughout the treatment.

Transmission electron microscopy (TEM) analysis of the zebrafish tendon

TEM of uninjured control and regenerated tendons (6 months post-injury) was performed at the Shriners Hospitals for Children in Portland, Oregon. A total of 3 control and 3 regenerated tendons were analyzed. Collagen fibril diameters from each sample were measured using Fiji. For each individual sample, 5-10 50,000x images across 3–4 different planes were blinded and analyzed through the injury site or the corresponding uninjured area in the control tendons. A total of ~6000–35000 fibrils were measured for each sample.

2-photon microscopy

For the time course imaging of *scxa:mCherry* fish, adults were euthanized as described above in order to immobilize the heart and pinned down onto an agarose plate with the mouth opened to allow for full extension of the tendon. The MST was imaged at 25x magnification at various time points pre- and post-injury. To visualize neutrophils, macrophages, and *scxa*-lineage cells, *mpx:eGFP*, *mpeg:eGFP, and scxa:creERT2;ubi:zebrabow* fish were euthanized and the heads were fixed overnight in 4% paraformaldehyde at 4 degrees. The tendons were then dissected out of the heads and stained overnight in Draq5 in 1% Triton-X/D-PBS. The stained tendons were embedded into 1% low melting point (LMP) agarose and imaged on the 2-photon. For all 2-photon imaging, a second harmonic generation signal was acquired and overlaid to visualize the tendon collagen matrix alignment.

EdU detection, immunostaining, and Masson's trichrome staining

Approximately 8–10 µL of 10 mM EdU solution were injected intraperitoneally (IP) into adult zebrafish 24 h prior to tissue collection. For whole mount EdU-staining, adult heads were fixed overnight in 4% paraformaldehyde at 4 degrees. The tendons were dissected out of the heads and permeabilized overnight in 1% Triton-X/D-PBS. Click-it EdU staining was then performed according to the manufacturer's instructions (Invitrogen) followed by Draq5 nuclear counterstaining and 2-photon imaging. For the combined lineage tracing and EdU staining on sections, adult tendons were dissected and fixed overnight in 4% paraformaldehyde at 4 degrees, brought up a gradient to 30% sucrose, and embedded into OCT. Samples were cryo-sectioned at 12 µm thickness and blocked for 1 h (8% donkey serum, 0.3% BSA, 1% Triton-X) prior to performing Click-it EdU staining. After EdU staining, immunostaining was performed with an anti-GFP antibody (1:250 dilution, Abcam Cat No. ab290) to stain for CFP/YFP labeled cells. Phospho-Smad3 staining was performed at a 1:250 dilution (Abcam Cat No. ab52903). Sections were then imaged using confocal microscopy under the same settings for each respective experiment. Masson's trichrome staining was performed according to the manufacturer's protocol (Sigma Aldrich).

Imaging quantification

For both the immune cell and EdU quantification across time points, 2–3 slices were extracted from the *z*-stacks of the whole mounted tendon tissue from individual animals. The images were processed to include only the injury area (i.e. between the two severed tendon ends), blinded, and the percentage of either *mpx:eGFP* +, *mpeg:eGFP* +, or EdU+ cells out of total Draq5+ cells in the injury site was quantified. The percentages across all sections for each sample were averaged. A one-way ANOVA statistical analysis was performed with Tukey's multiple comparisons tests to determine statistically significant changes across the dataset and between different time points. Defect size was quantified from *Z*-projected 2-photon stacks measuring the distance between both severed tendon ends (from SHG signal). For the quantification of *scxa*-lineage cells in the regenerating bridge at 14 dpi, 3–4 slices were isolated from 2-photon z-stacks per sample, and the percentage of CFP+/YFP+ cells in the injury site out of total Draq5+ cells were quantified. For the quantification of *scxa:mCherry*+ cells and *scxa*-lineage cells in the injury site following DMSO or SB-431542 treatment, 2-3 slices were isolated from 2-photon *z*-stacks per sample. The percentage of *scxa:mCherry*+ cells or stained CFP+/YFP+ cells (GFP+) in the mesenchymal portion of the injury site (out of Draq5+ nuclei, excluding the epithelial-like expansion) as well as the cell density (per 500 µm2) were quantified. For the quantification of EdU+ *scxa*-lineage cells in the tendon stubs and injury site, sections were processed in ImageJ to isolate the respective regions and the percentages of EdU/GFP co-positive and GFP+ cells were quantified (out of Draq5+ nuclei) from DMSO and SB-431542-treated samples (1–4 dpi treatment condition). For the tendon ends, the first 150 µm from the severed end were quantified. All imaging quantification was performed in a blinded manner except for the lineage contribution at 14 dpi during normal regeneration and the defect size with SB-431542 treatment.

Generation and validation of a TgBAC(*scxa:creERT2*) zebrafish line

To generate a *TgBAC(scxa:creERT2)* zebrafish line, standard BAC recombineering was performed to modify the *scxa*-containing BAC (CH211-251G8) from the CHORI BAC library to (1) include a *cryaa:sfGFP* in the backbone of the BAC for screening purposes and (2) introduce a creERT2 immediately after the *scxa* promoter. Briefly, to insert *cryaa:sfGFP* into the backbone of the BAC, the iTol2 flanked kanR-cryaa:sfGFP fragment was PCR amplified from Addgene #74153 (Fuentes et al., 2016) and electroporated into *scxa*-containing BAC containing cells. A successfully recombineered clone was identified and utilized for subsequent steps. To introduce the creERT2 sequence after the *scxa* promoter, a custom vector housing a creERT2-frt-ampR-frt fragment was first generated via Gibson assembly. The creERT2-frt-ampR-frt fragment was then amplified with primers containing homology arms for the *scxa* locus such that the insertion should occur directly into the ATG start site. The fragment was then recombineered into the *scxa* BAC with cryaa:sfGFP to generate the final *scxa:creERT2* BAC construct.

Wildtype Tübingen zebrafish eggs were injected at the 1 cell stage with the engineered *scxa:creERT2* BAC and *tol2* mRNA. Injected F0 larvae that displayed green lenses were grown to adulthood for germline transmission screening and validation of creERT2 labeling. To screen for potential founders, F0 adults were outcrossed to the *ubi:zebrabow* line and embryos were immersed in 20 µM 4-hydroxytamoxifen (4OH-T) beginning at 48 hpf. Developing larvae were screened at 72 hpf to identify founders that gave rise to progeny with labeled developing *scxa*+ tendon structures. Double *scxa:creERT2;ubi:zebrabow* embryos from promising founders were then raised to adulthood and dosed with 4OH-T to test for labeling in the adult MST. Of these, 3 stable founder lines were established all showing high specificity, but variable labeling efficiency during adulthood. Therefore, we moved forward with the founder line showing highest labeling efficiency for all subsequent experiments. To optimize labeling,

several routes of 4OH-T delivery were tested including immersion, IP injection, and local injection. Of these, the highest efficiency of labeling was determined to be via immersion.

Lineage tracing of adult *scxa:creERT2* zebrafish

Adult zebrafish (~5–6 months old) were immersed in 2.5 µM 4OH-T for 3 nights (~12 h per night) at a density of 100 mL per fish and protected from light. Between treatments, fish were placed into normal fish system water and fed daily. Following the conclusion of 4OH-T treatment, fish were returned to the normal system, and tendon injuries were performed at 7 or 14 days post-treatment depending on the experiment. Tissue was collected at designated time points (either 0, 4, 7, or 14 dpi depending on the experiment) and either imaged on the 2-Photon or processed for combined EdU/antibody staining (see prior section).

HCR and RNAscope in situ hybridization

Whole mount HCR double in situ hybridization of *scxa* and *cre* was performed on 4 dpf *scxa:creERT2* larvae according to the manufacturer's protocol with proteinase K treatment for 10 min at 10 µg/mL. RNAscope in situ hybridization of *scxa*, *tgfbr1b*, and *tgfbr2a* on cryosections was performed according to the manufacturer's protocol. When combining RNAscope in situ hybridization with immunostaining for detection of CFP/YFP, sections were directly blocked for 1 h at room temperature after the last HRP blocking step of the RNAscope protocol and then immunostaining was performed with an anti-GFP antibody (1:1000, Abcam, ab13970) as described above.

Reporting summary

Further information on research design is available in the Nature Research Reporting Summary linked to this article.

DATA AVAILABILITY

The authors declare that all the data generated in this study are available in the manuscript and supplemental information. Requests for reagents in the study should be directed to the corresponding author (jgalloway@mgh.harvard.edu).

Received: 9 January 2023; Accepted: 31 August 2023;
Published online: 19 September 2023

REFERENCES

1. Grinstein, M. & Galloway, J. L. in *Developmental Biology and Musculoskeletal Tissue Engineering* (eds J. M. Stoddart, A. M. Craft, G. Pattappa, & O. F. W. Gardner) Ch. 8, 181–206 (Academic Press, 2018).
2. Egerbacher, M., Gabner, S., Battisti, S. & Handschuh, S. Tenocytes form a 3-D network and are connected via nanotubes. *J. Anat.* **236**, 165–170 (2020).
3. Kalson, N. S. *et al*. A structure-based extracellular matrix expansion mechanism of fibrous tissue growth. *Elife* **4**. https://doi.org/10.7554/eLife.05958 (2015).
4. Chatterjee, M., Muljadi, P. M. & Andarawis-Puri, N. The role of the tendon ECM in mechanotransduction: disruption and repair following overuse. *Connect Tissue Res.* **63**, 28–42 (2022).
5. Mienaltowski, M. J., Gonzales, N. L., Beall, J. M. & Pechanec, M. Y. Basic structure, physiology, and biochemistry of connective tissues and extracellular matrix collagens. *Adv. Exp. Med. Biol.* **1348**, 5–43 (2021).
6. Subramanian, A. & Schilling, T. F. Tendon development and musculoskeletal assembly: emerging roles for the extracellular matrix. *Development* **142**, 4191–4204 (2015).
7. Nichols, A. E. C., Best, K. T. & Loiselle, A. E. The cellular basis of fibrotic tendon healing: challenges and opportunities. *Transl. Res.* **209**, 156–168 (2019).
8. Butler, D. L., Juncosa, N. & Dressler, M. R. Functional efficacy of tendon repair processes. *Annu. Rev. Biomed. Eng.* **6**, 303–329 (2004).
9. Tsai, S. L., Nodl, M. T. & Galloway, J. L. Bringing tendon biology to heel: leveraging mechanisms of tendon development, healing, and regeneration to advance therapeutic strategies. *Dev. Dyn.* **250**, 393–413 (2021).
10. Henke, K. et al. Genetically engineered zebrafish as models of skeletal development and regeneration. *Bone*, 116611. https://doi.org/10.1016/j.bone.2022.116611 (2022).
11. Kaji, D. A., Howell, K. L., Balic, Z., Hubmacher, D. & Huang, A. H. Tgfbeta signaling is required for tenocyte recruitment and functional neonatal tendon regeneration. *Elife* **9**. https://doi.org/10.7554/eLife.51779 (2020).
12. Howell, K. et al. Novel model of tendon regeneration reveals distinct cell mechanisms underlying regenerative and fibrotic tendon healing. *Sci. Rep.* **7**, 45238 (2017).
13. Arvind, V., Howell, K. & Huang, A. H. Reprogramming adult tendon healing using regenerative neonatal regulatory T cells. *bioRxiv*. https://doi.org/10.1101/2021.05.12.443424 (2021).
14. Niu, X., Subramanian, A., Hwang, T. H., Schilling, T. F. & Galloway, J. L. Tendon cell regeneration is mediated by attachment site-resident progenitors and BMP signaling. *Curr. Biol.*. https://doi.org/10.1016/j.cub.2020.06.016 (2020).
15. Chen, J. W. & Galloway, J. L. The development of zebrafish tendon and ligament progenitors. *Development* **141**, 2035–2045 (2014).
16. Grinstein, M. et al. A distinct transition from cell growth to physiological homeostasis in the tendon. *Elife* **8**. https://doi.org/10.7554/eLife.48689 (2019).
17. Gemberling, M., Bailey, T. J., Hyde, D. R. & Poss, K. D. The zebrafish as a model for complex tissue regeneration. *Trends Genet.* **29**, 611–620 (2013).
18. Shah, R. R., Nerurkar, N. L., Wang, C. C. & Galloway, J. L. Tensile properties of craniofacial tendons in the mature and aged zebrafish. *J. Orthop. Res.* **33**, 867–873 (2015).
19. Diogo, R., Hinits, Y. & Hughes, S. M. Development of mandibular, hyoid and hypobranchial muscles in the zebrafish: homologies and evolution of these muscles within bony fishes and tetrapods. *BMC Dev. Biol.* **8**, 24 (2008).
20. Koch, M. et al. A novel marker of tissue junctions, collagen XXII. *J. Biol. Chem.* **279**, 22514–22521 (2004).
21. Charvet, B. et al. Knockdown of col22a1 gene in zebrafish induces a muscular dystrophy by disruption of the myotendinous junction. *Development* **140**, 4602–4613 (2013).
22. Jacobson, K. R. et al. Comparative analysis of the extracellular matrix proteome across the myotendinous junction. *J. Proteome Res.* **19**, 3955–3967 (2020).
23. Petrany, M. J. et al. Single-nucleus RNA-seq identifies transcriptional heterogeneity in multinucleated skeletal myofibers. *Nat. Commun.* **11**, 6374 (2020).
24. Sanchez-Iranzo, H. et al. Transient fibrosis resolves via fibroblast inactivation in the regenerating zebrafish heart. *Proc. Natl Acad. Sci. USA* **115**, 4188–4193 (2018).
25. Gaut, L. & Duprez, D. Tendon development and diseases. *Wiley Interdiscip. Rev. Dev. Biol.* **5**, 5–23 (2016).
26. Brent, A. E., Schweitzer, R. & Tabin, C. J. A somitic compartment of tendon progenitors. *Cell* **113**, 235–248 (2003).
27. Pryce, B. A., Brent, A. E., Murchison, N. D., Tabin, C. J. & Schweitzer, R. Generation of transgenic tendon reporters, ScxGFP and ScxAP, using regulatory elements of the scleraxis gene. *Dev. Dyn.* **236**, 1677–1682 (2007).
28. Bobzin, L., Roberts, R. R., Chen, H. J., Crump, J. G. & Merrill, A. E. Development and maintenance of tendons and ligaments. *Development* **148**. https://doi.org/10.1242/dev.186916 (2021).
29. Nodl, M. T., Tsai, S. L. & Galloway, J. L. The impact of Drew Noden's work on our understanding of craniofacial musculoskeletal integration. *Dev. Dyn.* **251**, 1250–1266 (2022).
30. Meyers, C. et al. Heterotopic ossification: a comprehensive review. *JBMR* **3**, e10172 (2019).
31. Harvey, T., Flamenco, S. & Fan, C. M. A Tppp3(+)Pdgfra(+) tendon stem cell population contributes to regeneration and reveals a shared role for PDGF signalling in regeneration and fibrosis. *Nat. Cell Biol.* **21**, 1490–1503 (2019).
32. Wang, Y. et al. Osteocalcin expressing cells from tendon sheaths in mice contribute to tendon repair by activating Hedgehog signaling. *Elife* **6**. https://doi.org/10.7554/eLife.30474 (2017).
33. Grinstein, M. et al. A quiescent resident progenitor pool is the central organizer of tendon healing. *bioRxiv*. https://doi.org/10.1101/2022.02.02.478533 (2022).
34. Nichols, A. E., Wagner, N. W., Ketonis, C. & Loiselle, A. Epitenon-derived cells comprise a distinct progenitor population that contributes to both tendon fibrosis and regeneration following acute injury. *bioRxiv*. https://doi.org/10.1101/2023.01.30.526242 (2023).
35. Dyment, N. A. et al. Lineage tracing of resident tendon progenitor cells during growth and natural healing. *PLoS One* **9**, e96113 (2014).
36. Meng, X. M., Nikolic-Paterson, D. J. & Lan, H. Y. TGF-beta: the master regulator of fibrosis. *Nat. Rev. Nephrol.* **12**, 325–338 (2016).
37. Kallenbach, J. G. et al. Altered TGFB1 regulated pathways promote accelerated tendon healing in the superhealer MRL/MpJ mouse. *Sci. Rep.* **12**, 3026 (2022).
38. Pryce, B. A. et al. Recruitment and maintenance of tendon progenitors by TGFbeta signaling are essential for tendon formation. *Development* **136**, 1351–1361 (2009).
39. Tan, G. K. et al. Tgfbeta signaling is critical for maintenance of the tendon cell fate. *Elife* **9**. https://doi.org/10.7554/eLife.52695 (2020).

40. Havis, E. et al. TGFbeta and FGF promote tendon progenitor fate and act downstream of muscle contraction to regulate tendon differentiation during chick limb development. *Development* **143**, 3839–3851 (2016).
41. Subramanian, A., Kanzaki, L. F., Galloway, J. L. & Schilling, T. F. Mechanical force regulates tendon extracellular matrix organization and tenocyte morphogenesis through TGFbeta signaling. *Elife* **7**. https://doi.org/10.7554/eLife.38069 (2018).
42. Maeda, T. et al. Conversion of mechanical force into TGF-beta-mediated biochemical signals. *Curr. Biol.* **21**, 933–941 (2011). [pii] 10.1016/j.cub.2011.04.007.
43. Lee, J. H. & Massague, J. TGF-beta in developmental and fibrogenic EMTs. *Semin Cancer Biol.* **86**, 136–145 (2022).
44. Talbott, H. E., Mascharak, S., Griffin, M., Wan, D. C. & Longaker, M. T. Wound healing, fibroblast heterogeneity, and fibrosis. *Cell Stem Cell* **29**, 1161–1180 (2022).
45. Kardon, G. Muscle and tendon morphogenesis in the avian hind limb. *Development* **125**, 4019–4032 (1998).
46. Brent, A. E., Braun, T. & Tabin, C. J. Genetic analysis of interactions between the somitic muscle, cartilage and tendon cell lineages during mouse development. *Development* **132**, 515–528 (2005).
47. McGurk, P. D., Swartz, M. E., Chen, J. W., Galloway, J. L. & Eberhart, J. K. In vivo zebrafish morphogenesis shows Cyp26b1 promotes tendon condensation and musculoskeletal patterning in the embryonic jaw. *PLoS Genet* **13**, e1007112 (2017).
48. Yuan, H. et al. Sumoylation of CCAAT/enhancer-binding protein alpha promotes the biased primitive hematopoiesis of zebrafish. *Blood* **117**, 7014–7020 (2011).
49. Ellett, F., Pase, L., Hayman, J. W., Andrianopoulos, A. & Lieschke, G. J. mpeg1 promoter transgenes direct macrophage-lineage expression in zebrafish. *Blood* **117**, e49–e56 (2011).
50. Pan, Y. A. et al. Zebrabow: multispectral cell labeling for cell tracing and lineage analysis in zebrafish. *Development* **140**, 2835–2846 (2013).

ACKNOWLEDGEMENTS

We would like to thank Sara Tufa and Doug Keene at the Shriners Hospital for Children in Portland, Oregon for their help with performing the TEM. We would also like to thank our funding sources for this work: S.L.T. was supported by the Helen Hay Whitney Foundation (HHWF) Postdoctoral Fellowship. S.V., R.R.S., and J.L.G. were supported by the Harvard Stem Cell Institute, NIH/NIAMS AR074541 and AR079495. The funding sources played no role in study design, data collection, analysis and interpretation of data, or the writing of this manuscript.

AUTHOR CONTRIBUTIONS

S.L.T., R.R.S., and J.L.G. conceptualized the study design. S.L.T. performed all the experiments, data analysis, and wrote the manuscript. S.V. assisted in generating the *Tg(scxa:creERT2)* line, TEM analysis, and image quantification. S.V., R.R.S., and J.L.G. revised the manuscript. All authors approved the final manuscript.

COMPETING INTERESTS

The authors declare no competing interests.

ADDITIONAL INFORMATION

Supplementary information The online version contains supplementary material available at https://doi.org/10.1038/s41536-023-00328-w.

Correspondence and requests for materials should be addressed to Jenna L. Galloway.

Reprints and permission information is available at http://www.nature.com/reprints

Publisher's note Springer Nature remains neutral with regard to jurisdictional claims in published maps and institutional affiliations.